

EFFECT OF CONNECTION NONLINEARITY ON WIND PERFORMANCE OF TALL MASS TIMBER BUILDINGS

Chi ZHANG¹, Yuxin PAN²

ABSTRACT: Mass timber products have gained significant recognition in the construction of tall buildings, providing a sustainable solution for urban development. As those products have shown high in-plane strength and stiffness, energy dissipation and ductility of lightweight and flexible tall mass timber structures under lateral loads rely on metal connectors (e.g., hold-downs, shear brackets, and spline joints). Those connectors are commonly modeled as nonlinear springs in conventional seismic analysis but are often simplified as linear in serviceability wind assessment. However, under extreme wind hazards, excessive wind-induced vibrations may cause these connections to enter the nonlinear stage. This paper aims to investigate the impact of nonlinear connections on the wind performance of tall mass timber buildings. To improve the efficiency of traditional discrete connectors modeling in cross-laminated timber (CLT) wall panels, a novel “nonlinear connection zone” modeling approach is proposed to integrate all connectors into a continuous shell strip. The modelling method is first calibrated and validated with full-scale CLT shear wall tests with both single-panel and double-panel configurations. Next, the method is applied to a 30-story mass timber building using numerical fluid-structure interaction technology at extreme wind intensity. The analysis results showed that the case-study building exhibited nonlinear behavior at the design wind speed with a return period of 1,000 years, and neglecting nonlinearity would underestimate the peak response.

KEYWORDS: *mass timber building, CLT, metal connector, nonlinear modeling, wind-induced vibrations*

1 – INTRODUCTION

Mass timber materials, incorporating advanced engineered wood products such as cross-laminated timber (CLT) and glued laminated timber (glulam), offer a sustainable and compelling solution for constructing tall buildings. Mass timber construction boasts exceptional structural properties, including a high strength-to-weight ratio and construction flexibility, while outperforming traditional concrete and steel alternatives in terms of carbon sequestration throughout the entire building life cycle [1].

As buildings ascend to greater heights, the inherent characteristics of tall mass timber structures, such as their relatively lower mass and increased flexibility, render them more susceptible to lateral loads like earthquakes and wind-induced vibrations. Lateral loads primarily induce deformations in the connections with prefabricated CLT panels used for floors, walls, and roofing, exhibiting rigid behavior [2]. In conventional seismic analysis, connectors are typically modeled as nonlinear to account for energy

dissipation at large deformation under reversed dynamic loading, while in the context of wind-induced vibrations, connectors are often assumed to behave linearly based on the serviceability assumption. Nevertheless, it is important to acknowledge that under extreme wind hazards, the wind-induced vibrations experienced by high-rise buildings can reach significant magnitudes, leading to nonlinear behavior of the connectors [3].

Mass timber connections typically consist of a combination of metal brackets, angles, screws, and nails. The prevalent approach for modeling those connections with nonlinear response involves using discrete connector elements with specified properties [4]. Referring to Fig. 1a and 1b, the vertical spring elements simulate hold-downs and the horizontal spring elements simulate shear brackets. The number of these metal elements can be substantial as CLT buildings are often constructed with hundreds of thousands of screws. The large quantity of connecting elements poses challenges in developing accurate prediction models for their behavior - the placement of

¹ Chi ZHANG, Department of Civil and Environmental Engineering, The Hong Kong University of Science and Technology, Hong Kong, China, czhangdt@connect.ust.hk

² Yuxin PAN, Department of Civil and Environmental Engineering, The Hong Kong University of Science and Technology, Hong Kong, China, ceypan@ust.hk

nonlinear connector elements throughout the building is cumbersome and makes the model difficult to converge.

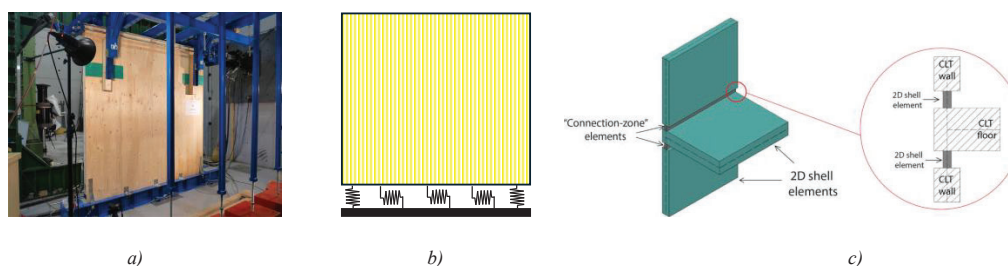


Figure 1. a) Standard single-panel shear wall [5]; b) schematic diagram of discrete connector elements, and c) original CZS method [6]

Some efforts have been made to simplify this procedure. Tulebekova et al. [6] proposed a “linear connection zone (LCZ)” shell to represent the wall-to-floor discrete connectors in the numerical model of CLT buildings. In this method, as seen in Fig. 1c, a group of connectors at the base of the shear wall is replaced with a continuous strip shell area. The material properties of the LCZ are the same as the CLT wall, but the mechanical properties of the connector are reflected by uniformly reducing the thickness of the LCZ (typically 8% of the original wall thickness). Although this method worked for certain walls, there was a limitation that lies in the uniform decrease in strength by the reduction in thickness in all directions (horizontal shear, vertical uplift, and vertical compression), which diverges from reality with coupled axial-shear properties and low vertical compression capacity. In rocking kinematic motion of the CLT shear wall, the anti-uplift connectors (hold-downs) and shear connectors (angle brackets) provide resistance and stiffness in the vertical tensile and horizontal shear directions, while the strength in the vertical compression direction is provided by the CLT wall itself. Consequently, the LCZ should exhibit asymmetric tension-compression characteristics. A similar study was conducted by Christovasilis et al. [7], where they utilized orthotropic continuous shell elements to simulate the shear connectors. This was achieved by adjusting the in-plane shear modulus in the material constitutive matrix of the LCZ shell, maintaining the same thickness as the wall. It was argued that under small lateral loads, the shearwall primarily exhibits sliding without considering the rocking behavior. While this approach enhances the efficiency of connection modeling, it is limited to linear and pure sliding assumptions. Later, Rinaldi et al. [8] updated this model with by accounting for the combined rocking-sliding motions. When the overturning moment caused by the lateral load surpasses the stable moment produced by the gravity load, the CLT wall enters the combined rocking-sliding stage.

Subsequently, Young’s modulus of the LCZ shell in the vertical uplift direction is determined by the tensile stiffness of the anti-uplift member instead of the material properties of CLT. Despite the advancement, this model still presents some limitations: a) it is challenge to accurately determine the deformation stage of different shear walls under actual load conditions throughout an entire building; b) the tension-compression asymmetric characteristics of the connection shell material remain unsolved; and c), this approach still hinges on a linear assumption.

To address those limitations, this study proposes a novel “nonlinear connection zone (NCZ)” model, aiming to assess the nonlinear behavior of the CLT buildings under extreme lateral loads, including strong wind conditions. The proposed model can effectively capture the tension-compression asymmetric characteristics and the nonlinear behavior at the connection zone, integrating various types of connectors, and ultimately, reducing the complexity of numerical simulations. After validation against full-scale CLT shear wall testing, this method is applied to a 30-story case-study mass timber building. The analysis employs fluid-structure interaction (FSI) techniques, integrating computational fluid dynamics (CFD) and finite element (FE) analysis.

2 – METHODOLOGY

2.1 Problem Formulation

The kinematic modes of CLT shear walls induced by the connections primarily include rocking and sliding, as shown in Fig. 2a. Rocking behavior is predominantly governed by hold-downs, while sliding behavior is controlled by angle brackets. It can also cause shearing, compressing, and splitting at the panel-to-panel splint joints (see Fig. 2b).

To account for the plastic stage behavior, an ideal elastic-plastic (IEP) model is incorporated to replicate the connector's behavior beyond yielding, as shown in Fig. 3a and 3b. This ideal load-displacement relationship of connectors is described by the equivalent-energy elastic-plastic (EEEP) procedure specified in ASTM E2126 [10] with the yield point (displacement d_y and strength F_y) and elastic stiffness ($K_e = F_y/d_y$). Therefore, the yield stress and strain of the material IEP model can be determined according to the connector's yield load F_y and yield displacement d_y .

The panel-to-panel connections, illustrated as a blue strip in Fig. 2b, can experience compression, splitting, and shear deformation. Therefore, there is also a tension-compression asymmetry in the anti-splitting direction. The IEP material model is also employed in this scenario. Typically, panel-to-panel connections are fastened with evenly spaced screws, which control the adjustment of the modulus and the determination of the yield point.

2.2 Wall application

This section demonstrates the proposed model using a single-panel wall (Fig. 1a) as an example, with two hold-downs at the bottom corners and n angle brackets. K_T , d_y are the elastic stiffness and yield displacement of the hold-down, while K_s , v_y denote the elastic stiffness and yield displacement of the angle bracket. A NCZ shell strip is introduced to replace these connectors. In the rocking mode, the deformed part of the NCZ shell strip is in the shape of a red triangle, and in the sliding mode, the deformed part of the NCZ shell strip is in the shape of a red parallelogram, as shown in Fig. 1b. The strain is assumed to be uniform along the strip height.

When the shear wall undergoes rocking, in the elastic stage, by equilibrium, the force generated by the internal stress within the red deformed triangle (Fig. 2a) equals to the anti-lift force supplied by the hold-down. Thus, the tension elastic modulus E_1^T of the continuous shell material is determined as Equation (3). The compression modulus E_1^C is equal to the elastic modulus of the CLT (E_1^{CLT}) in this direction, see Equation (4). In the plastic stage, the internal stress is regarded as the yield stress when the uplift height of the red deformed triangle is equivalent to the yield displacement (u_y) of the hold-down connector. Therefore, the tensile yield strain ε_{1yield}^T and stress σ_{yield}^T can be calculated by Equation (5) and (6), respectively. This assumption introduces an increased stiffness at the onset of the plastic stage. As the red triangular deformation area yields gradually from the leftmost end to the right, the

unyielded portion within this area contributes additional stiffness.

$$E_1^T = K_T \frac{2h}{lt} \quad (3)$$

$$E_1^C = E_1^{CLT} \quad (4)$$

$$\varepsilon_{1yield}^T = \frac{u_y}{h} \quad (5)$$

$$\sigma_{1yield}^T = E_1^T \frac{u_y}{h} \quad (6)$$

When the shear wall undergoes sliding, in the elastic stage, the shear stiffness arising from the internal shear stress within the red deformed parallelogram (Fig. 2a) equals to the stiffness provided by the angle brackets. The shear modulus G_{12} of the continuous shell material is calculated as Equation (7). In the plastic stage, the internal shear stress is considered as the yield shear stress when the offset length of the upper and lower sides of the red deformed parallelogram matches the yield displacement (v_y) of the shear bracket connector. Therefore, the shear yield strain $\gamma_{12yield}^T$ and stress $\tau_{12yield}^T$ can be determined by Equation (8) and (9), respectively.

$$G_{12} = nK_s \frac{h}{lt} \quad (7)$$

$$\gamma_{12yield}^T = \frac{v_y}{h} \quad (8)$$

$$\tau_{12yield}^T = G_{12} \frac{v_y}{h} \quad (9)$$

Regarding the panel-to-panel connections, the equations for the elastic modulus, yield strain and stress (Equation (10)-(14)) are similar to those for the wall-to-floor connection, except for the elastic modulus E_2^T in the anti-splitting direction. Since evenly spaced screws can ensure consistent anti-splitting stiffness across the connection area, the tensile modulus (E_2^T) is calculated using Equation (10), where K_{sc} represents the total stiffness of all the screws, l , h , t are the geometric parameters of the panel-to-panel NCZ shell strip (see Fig. 2b), and w_y is the yield displacement of the screw.

$$E_2^T = K_{sc} \frac{h}{lt} \quad (10)$$

$$E_2^C = E_2^{CLT} \quad (11)$$

$$\sigma_{2yield}^T = E_2^T \frac{w_y}{h} \quad (12)$$

$$G_{12} = K_{sc} \frac{h}{lt} \quad (13)$$

$$\tau_{12yield}^T = G_{12} \frac{w_y}{h} \quad (14)$$

Based on the derivations above, the proposed method uses a nonlinear tensile-compression asymmetric continuous shell strip to replace connector groups. The sliding and

rocking behaviors of CLT shear walls can be simulated by adjusting the material constitutive matrix combined with the IEP model.

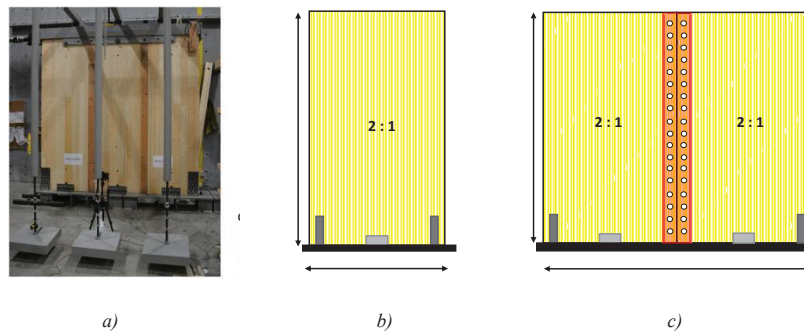


Figure 4. a) Experimental setup [4], b) single-panel wall configuration, c) couple-panel wall configuration

3 – VALIDATION OF THE PROPOSED METHOD

The proposed method is validated based on monotonic tests of both a single panel and a coupled panel [4]. The test setup is illustrated in Fig. 4a. The CLT panel has a strength grade of 191V2 [11] and consists of five layers with a thickness of 139 mm (35×17×35×17×35). The equivalent elastic modulus are 8400 MPa in the vertical direction, 2970 MPa in the horizontal direction, and the shear modulus is 690 MPa. The CLT panel has an aspect ratio of 2:1, measuring 3 m in height and 1.5 m in width.

In the single-panel configuration shown in Fig. 4b, two hold-downs are placed at the bottom corners, with an angle bracket positioned in the center. For the coupled panel depicted in Fig. 4c, a hold-down is located at the bottom of each side, and an angle bracket is situated in the middle of each panel, resulting in a total of two angle brackets. The coupled panels are connected using spline joints. The hold-downs and angle brackets are secured to the CLT panel with 11 and 8 ASSY Kombi LT screws (Ø12 × 120 mm), respectively. The spline joint is fastened with 19 ASSY Eco screws (Ø8 × 100 mm). Lateral loads were applied using a 250-kN actuator located at the top of the

left wall panel, with a displacement-controlled rate of 15 mm/min. Additionally, a vertical gravity load of 10 kN/m was applied at the top of the wall, simulating a moderately loaded wall in a two-story system. According to [4], the elastic stiffness of the hold-down is 16.1 kN/mm, with a yield displacement of 11.7 mm. The angle bracket has an elastic stiffness of 11.7 kN/mm and the same yield displacement of 11.7 mm. The spline exhibits an elastic stiffness of 14.3 kN/mm, with a yield displacement of 6.1 mm. Using Equations (1)-(14), the corresponding elastic modulus and shear modulus were calculated in Table 1. The yield stress for anti-uplift or anti-splitting (σ_{yield}^T) and the in-plane shear yield stress (τ_{yield}^T) were also calculated.

ANSYS [12] is adopted to simulate the monotonic tests of single and coupled panels using the proposed NCZ method. The user material subroutine was then employed to create an IEP tension-compression asymmetric orthotropic material. Fig. 5a illustrates the deformation of the single panel under a 100 kN lateral load and the coupled panel under a 150 kN lateral load. The NCZ shell demonstrates clear tension-compression asymmetry and shear deformation, effectively capturing the rocking and sliding behavior of the panels.

Table 1: NCZ Material Parameters for shear wall tests

Connection type		E_1^T (Mpa)	E_1^C (Mpa)	E_2^T (Mpa)	E_2^C (Mpa)	G_{12} (Mpa)	σ_{yield}^T (Mpa)	τ_{yield}^T (Mpa)
Wall-to-floor connection	Single panel	10.8	8400	2970		3.9	1.8	0.7
	Coupled panel	5.4	8400	2970		3.9	0.9	0.7
Panel-to-panel connection		8400		2.4	2970	2.4	0.2	0.2



Figure 5. a) Deformation diagram of finite element model, b) Comparison of model and monotonic test result

Fig. 5b compares the finite element simulation results with the experimental data. Since the material model parameters for the NCZ are derived from the EEEP curve of the connector, the experimental EEEP curve, shown as the red line, is obtained from the experimental backbone curve. For the single panel, the numerical model (blue line) aligns well with the experimental backbone and EEEP curves in the initial linear stage. The verification results show an acceptable trend and accuracy, with the numerical findings for maximum force capacity closely matching the experimental EEEP curve. However, as the analysis progresses into the plastic stage, the numerical results indicate higher stiffness than the experimental results. This increase in stiffness at the onset of the plastic stage is attributed to the setting of the material yield point in the E_1 direction, as noted in Section 2. For the coupled panel, the numerical model demonstrates satisfactory results with the experimental EEEP curve. The three curves are consistent in the initial linear stage, but both the EEEP curve and the numerical results exhibit greater stiffness than the backbone curve in the plastic stage.

4 – CASE STUDY: STRONG WINDS ON TALL MASS TIMBER BUILDING

4.1 Model and Analysis

To demonstrate the effectiveness of the proposed approach for wind assessment, a tall mass timber building was selected. The SOM building [13], designed for Chicago, USA, reaches a height of 102 meters and consists of 30 stories. It features a rectangular floor plan measuring 42 meters by 30 meters. The load-resisting system for each floor includes eighteen glulam columns at the perimeter, four CLT shear walls, two CLT cores, and reinforced concrete spandrels and link beams, with CLT floor elements securely fastened. The CLT floors are 245 mm thick (comprising 7 layers) and graded as E1M5. The CLT shear walls and core walls are 315 mm thick (comprising 9 layers) and also graded as E1M5. The equivalent elastic moduli are 6276 MPa in the vertical direction, 5095 MPa in the horizontal direction, and the shear modulus is 690 MPa.

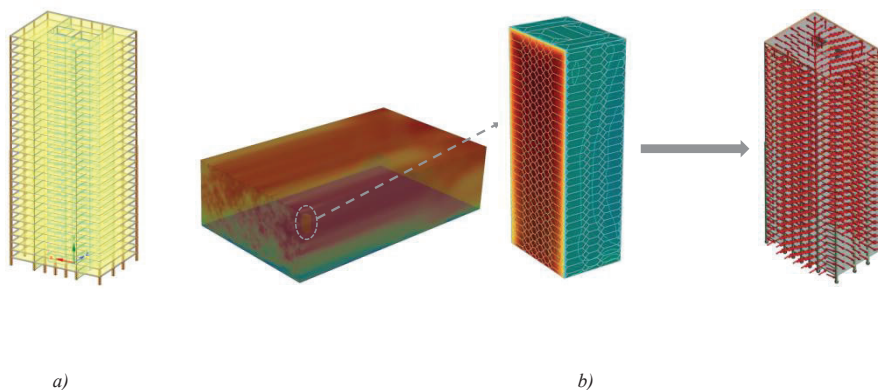


Figure 6. a) 3D view of the SOM building, b) Frame-distributed mapping method on SOM building.

Based on the wall-to-floor and panel-to-panel connection configurations for each CLT shear and core wall outlined in previous research [14], the corresponding elastic modulus and shear modulus for the NCZ method (represented by the blue shell strips in Fig. 6a) are

calculated, as presented in Table 2. In total, 3,360 wall-to-floor connectors and 600 splines were simplified to 1,440 NCZ shell strips, and only four user-defined materials were introduced.

Table 2: NCZ Material Parameters for Case-Study Building

Connection type		E_1^T (Mpa)	E_1^C (Mpa)	E_2^T (Mpa)	E_2^C (Mpa)	G_{12} (Mpa)	σ_{yield}^T (Mpa)	τ_{yield}^T (Mpa)
Wall-to-floor connection	Shear wall	109.1	6276	5095		190.9	1.4	2.4
	Core wall (shorter side)	180	6276	5095		175.0	2.7	2.2
	Core wall (longer side)	105.9	6276	5095		185.3	1.3	2.35
Panel-to-panel connection		6276		18.7	5095	18.7	0.6	0.6

Following the numerical wind tunnel guidelines [15], a 1:200 scale large eddy simulation wind tunnel was established in ANSYS Fluent, as shown in Fig. 6b. Based on the location of the prototype building, the 50-year local design wind speed at a reference height of 10 m is 22.95 m/s as per ASCE 7-10 standards [16]. To investigate the wind response under extreme conditions, a wind hazard with a return period of 1,000 years is considered in this study, and the corresponding wind speed is calculated to be 29.8 m/s, according to Equation (15) [17],

$$\frac{v_T}{v_{50}} = 0.36 + 0.1 \ln(12T) \quad (15)$$

where v_T , v_{50} are wind speeds with a return period of T and 50 years. The frame distribution pressure mapping technique [20] was then applied to transfer the pressure data obtained from the Numerical Wind Tunnel (NWT) to the outer frame of the building in the case study, as depicted in Fig. 6b. This mapping approach is noted for its computational efficiency and engineering accuracy.

In the structural dynamic analysis, the time history analysis method was employed, incorporating both the extreme wind load and the self-weight load. The total calculation duration was set to 150 seconds, with the final stabilized 100 seconds being recorded. Connection details were addressed using two methods:

- Method 1 (M1) follows the connection technique proposed by Christovasilis et al. [7], which operates under linear assumptions and considers only the sliding behavior of the CLT shear wall.
- Method 2 (M2) utilizes the proposed NCZ method to account for both the rocking and sliding behavior of the CLT shear wall.

4.2 Results and Discussions

The average displacement and acceleration time history curves at the roof floor for both M1 and M2 were extracted for comparison. Fig. 7 first presents the average displacement time history curves in both the along-wind and cross-wind directions. Due to the consideration of nonlinear effects in M2, there is a time shift of approximately 0 to 2 seconds in the displacement response waveforms compared to the linear results of M1. This is observed as an overall backward shift of the peak along the time axis. In terms of peak response displacement, M2 shows larger values than M1, with a maximum along-wind displacement of 210 mm for M2 and 189 mm for M1, and a maximum cross-wind displacement of 55 mm for M2 compared to 51 mm for M1. Thus, M1 underestimates the peak displacement responses, as it cannot account for nonlinearity.

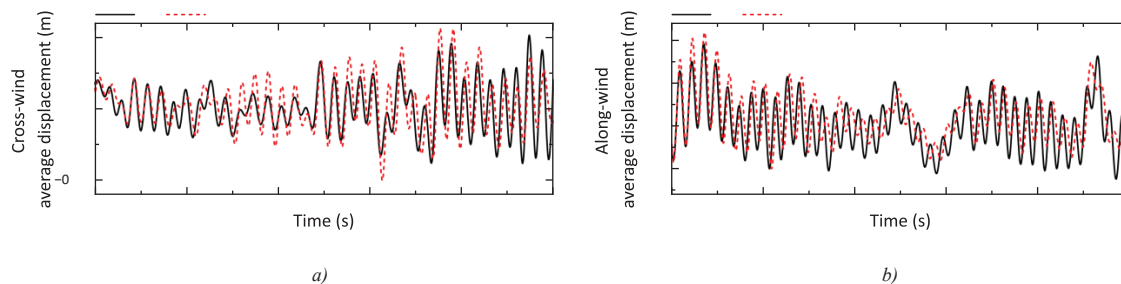


Figure 7. Average displacement at the roof floor: a) cross-wind, b) along wind

Fig. 8 shows the average acceleration time history curves in both directions. Similar to the observations in the

displacement response, M2 also exhibits a time shift in its acceleration response. The maximum along-wind

acceleration for M2 is greater than that for M1, measuring 0.33 m/s^2 for M2 and 0.26 m/s^2 for M1. The maximum cross-wind acceleration for both methods is similar, around 0.20 m/s^2 . Consequently, using M1 also leads to an underestimation of the peak acceleration responses.

It can be observed that the cross-wind response of M2 is generally greater than that of M1, while the along-wind response is similar for both, with M1 occasionally

exceeding M2. This indicates that for smaller cross-wind responses in frequency and amplitude, the stiffness degradation after yielding leads to the response of M2 exceeding that of M1. For along-wind responses with higher frequency and amplitude, the effects of nonlinear energy dissipation gradually become more pronounced. As a result, the acceleration response of M2 becomes lower than that of M1.

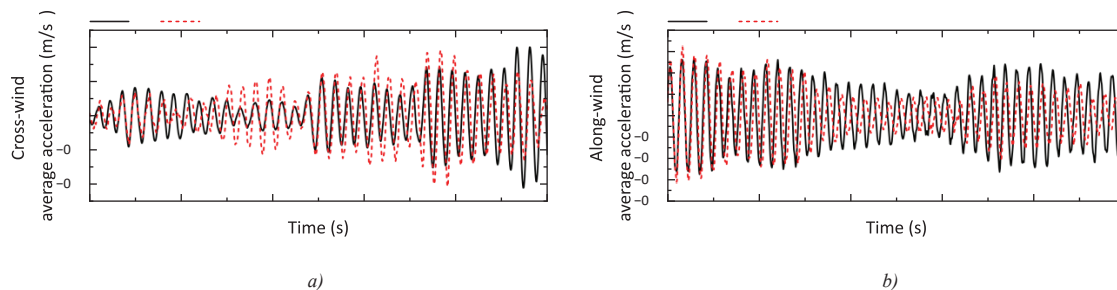


Figure 8. Average acceleration at the roof floor: a) cross-wind, b) along wind

5 – CONCLUSION

This study introduces an efficient nonlinear connection zone (NCZ) model for assessing wind loads on tall mass timber buildings. The model is experimentally validated and applied to a case study of a 102 m tall timber structure. A comparison was conducted between a linear pure-sliding connection method (M1) and the proposed NCZ method (M2). The following conclusions can be drawn:

- The experimental validation demonstrates that the proposed model closely matches the results from monotonic tests of both single-panel and couple-panel walls. The model can accurately simulate the rocking and sliding behaviors of the shear walls.
- Due to the nonlinear characteristics, M2 exhibits a time shift (up to 2 seconds) in displacement and acceleration responses when compared to M1.
- Without accounting for the nonlinearity, M1 underestimates the peak responses, with the maximum difference occurring in the along-wind direction. The peak acceleration and displacement of M2 in that direction are 210 mm and 0.33 m/s^2 , while M1 has 189 mm and 0.26 m/s^2 , respectively.
- The cross-wind response of M2 generally outperforms that of M1 due to the stiffness degradation, while M1 occasionally exceeds M2 in the along-wind responses because of the nonlinear energy dissipation.

The proposed method is both efficient and user-friendly, effectively capturing the rocking and sliding behaviors of CLT shear walls while incorporating nonlinearity. This approach allows engineers to quickly develop reliable finite element models that consider practical applications.

It is worth mentioning that the method currently focuses on the backbone curve, without accounting for the hysteretic behavior (e.g., pinching and cyclic degradation). Future research will focus on integrating those hysteretic behavior into the nonlinear models to enhance their accuracy. The authors' team is currently working on this task.

6 – ACKNOWLEDGEMENT

This research was supported by the Research Grants Council of the Hong Kong Special Administrative Region, China (Project No. 26204623) and the National Natural Science Foundation of China (Grant No. 52308280).

7 – REFERENCES

- [1] Y. Pan, M. Shahnewaz, T. Tannert, 2023. "Seismic performance and collapse fragility of balloon-framed CLT school building". In: *Journal of Earthquake Engineering* 27 (2023), pp. 3115-3135.
- [2] I. Gavric, M. Fragiaco, A. Ceccotti, 2015. "Cyclic behavior of CLT wall systems: Experimental tests and analytical prediction models". In: *Journal of structural engineering* 141 (2015), pp. 04015034.
- [3] N.K. Berile, M.A. Bezabeh, 2025. "Performance-based wind design of tall mass timber buildings with coupled post-tensioned cross-laminated timber shear walls". In: *Journal of Wind Engineering and Industrial Aerodynamics* 257 (2025), pp. 105981.
- [4] Y. Pan, T. Teflissi, T. Tannert, 2024. "Experimental Parameter Study on CLT Shear Walls with Self-Tapping



- Screw Connections”. In: *Journal of Structural Engineering* 150 (2024), pp. 04023192.
- [5] A. Aloisio, F. Boggian, R. Tomasi, et al., 2021. “The role of the hold-down in the capacity model of LTF and CLT shear walls based on the experimental lateral response”. In: *Construction and Building Materials* 289 (2021), pp. 123046.
- [6] S. Tulebekova, K.A. Malo, A. Rønquist, 2023. “Dynamic identification and model calibration of connection stiffness in multi-storey cross-laminated timber buildings”. In: *Journal of Building Engineering* 72 (2023), pp. 106607.
- [7] I. Christovasilis, L. Riparbelli, G. Rinaldin, et al., 2020. “Methods for practice-oriented linear analysis in seismic design of Cross Laminated Timber buildings”. In: *Soil Dynamics and Earthquake Engineering* 128 (2020), pp. 105869.
- [8] V. Rinaldi, D. Casagrande, C. Cimini, et al., 2021. “An upgrade of existing practice-oriented FE design models for the seismic analysis of CLT buildings”. In: *Soil Dynamics and Earthquake Engineering* 149 (2021), pp. 106802.
- [9] ANSI, 2018. “ANSI/APA PRG 320: Standard for Performance-Rated Cross-Laminated Timber”. In: American National Standards Institute. New York (NY) (2018).
- [10] E. ASTM, 2005. “Standard test methods for cyclic (reversed) load test for shear resistance of walls for buildings”. In: (2005).
- [11] CSA(Canadian Standard Association). 2019. *Engineering design in wood. CSA O86-19*. Mississauga, Canada: CSA., In.
- [12] ANSYS, 2017. *Ansys® Academic Research Mechanical*.
- [13] Skidmore, Owins, Merrill (SOM), 2013. *Timber Tower Research Project*. http://www.som.com/ideas/research/timber_tower_research_project. (August 2017).
- [14] M.A. Bezabeh, G.T. Bitsuamlak, M. Popovski, et al., 2018. “Probabilistic serviceability-performance assessment of tall mass-timber buildings subjected to stochastic wind loads: Part I-structural design and wind tunnel testing”. In: *Journal of Wind Engineering and Industrial Aerodynamics* 181 (2018), pp. 85-103.
- [15] A. Mochida, Y. Tominaga, R. Yoshie, 2006. *AIJ guideline for practical applications of CFD to wind environment around buildings*, 4th International Symposium on Computational Wind Engineering (CWE2006).
- [16] ASCE, 2010. *Minimum Design Loads for Buildings and Other Structures*, vol. 7. ASCE, Reston, VA.
- [17] J.A. Peterka, S. Shahid, 1998. “Design gust wind speeds in the United States”. In: *Journal of Structural Engineering* 124 (1998), pp. 207-214.
- [18] Engineering Sciences Data Unit (ESDU), 1974. *Characteristics of Atmospheric Turbulence Near the Ground*, Data Item 74031 ed.
- [19] H. Aboshosha, A. Elshaer, G.T. Bitsuamlak, et al., 2015. “Consistent inflow turbulence generator for LES evaluation of wind-induced responses for tall buildings”. In: *Journal of Wind Engineering and Industrial Aerodynamics* 142 (2015), pp. 198-216.
- [20] C. Zhang, Y. Pan, 2024. “Numerical Wind Dynamic Assessment of Tall Mass Timber Building Using Fluid-Structure Interaction Method”. In: Available at SSRN 5026924 (2024).